# 3상 조류 계산을 위한 Photovoltaic 시스템 모델

라이언 디올라타 송화창*
군산대학교 전자정보공학부

# Model of Photovoltaic Systems for 3 Phase Power Flow

Ryan Diolata and Hwachang Song
Kunsan National University

**Abstract** - Three phase power flow is commonly considered exclusively for the distribution systems, where single or double phase circuits may be present and loads may not always balanced between the three phases. This paper deals with modelling and analysis of grid connected photovoltaic (PV) system in three-phase power flow, with the consideration of the PV inverter output power limitations.

## 1. Introduction

The voltaic effect of the solar light is applied mostly in the three aspects: DC power supply, AC power supply of stand-alone inverters and grid connected inverters. The main components of a grid connected PV system includes series/parallel connection of the available PV panels and a power conditioning system in charge to extract and properly transfer the maximum available power present at the PV generator to the grid. To properly transfer this available power to the grid power flow analysis is needed.

In low voltage distribution system, there are unbalanced three-phase loads, in addition there are one-phase or two-phase lines in the distribution systems network. Loads in urban areas are mostly of the single phase type, fed from single phase feeders. In aggregate, this causes load and voltage unbalance in the system. Under this unbalanced operating conditions, three-phase power flow analysis are needed to assess the realistic operating conditions of the system. Three phase power flow is commonly considered exclusively for the distribution systems, where single or double phase circuits may be present and loads may not always balanced between the three phases.

In this paper, the grid connected PV system is modeled in three-phase power flow by taking into account the limitations on the inverter output power rating.

## 2. PV System

### 2.1 PV Power Model

To utilize solar energy as electrical energy basic components are required. Such that, solar panels, DC-AC converters (i.e. inverter), sensors and controls (i.e. Maximum Power Point Trackers). Fig. 1 shows the grid connected PV system and its components.

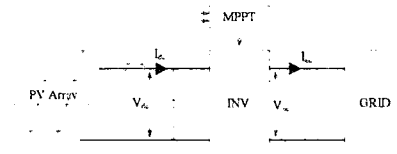


Fig. 1 PV Inverter System for Utility applications

The PV arrays are arranged in series/parallel to acquire the suitable power and voltage. Maximum power point tracker (MPPT) is used to maximize the power drawn from PV modules under varying atmospheric conditions. Also, the MPPT controls the inverter to produce the maximum power and ac power to be connected to load or utility grid.

From [1], the proposed I-V characteristic model equation (1) takes into consideration the percentage of effective intensity of the light over the solar panels, the characteristic constant for the I-V curves, a shading linear factor, the short-circuit current rating and the open-circuit voltage for each panel.

$$I_{ac} = \alpha * I_{\alpha} * \left[1 - \exp\left(\frac{V}{\kappa*(\lambda*\alpha+1-\lambda)*V_{oc}} - \frac{1}{\kappa}\right)\right] \qquad (1)$$

where $I_{ac}$ is the PV inverter total output current. $V$ is the voltage of operation for PV inverter system. $\alpha$ is the percentage of effective intensity of the light over the solar panels, (i.e. 100% of intensity of light over the solar panels is $\alpha = 1$). *Voc* is the open circuit voltage rating of the solar panels array for an effective intensity of light of 100% over the solar panels. *Isc* is the short circuit current rating of the solar panels array. *Iα* depends on *Isc*, with the relationship shown in (2). $\lambda$ is the linear shading factor depending on *Voc*, as defined in (3). *Vmin* is the open-circuit voltage rating of the solar panels array for a minimum intensity of light over the solar panels. $K$ is the exponential I-V characteristic constant.

$$I_{\alpha} = \frac{I_{sc}}{\alpha - \alpha * \exp\left(\frac{-1}{K}\right)} \qquad (2)$$

$$\lambda = \frac{V_{oc} - V_{min}}{V_{oc}} \qquad (3)$$

To obtain the P-V characteristic equation (1) is multiplied by $V$. The resulting equation (4) defines the inverter output power for different intensities of light. To approximate the maximum power output of the inverter, *Vα* from (5) is substituted in (4).

$$P = V * \left[\alpha * I_{\alpha} * \left[1 - \exp\left(\frac{V}{\kappa*(\lambda*\alpha+1-\lambda)*V_{oc}} - \frac{1}{\kappa}\right)\right]\right] \qquad (4)$$

$$V_{\alpha} = V_{oc} * (\lambda*\alpha*+1-\lambda) * \left[1 + \kappa * \ln\left(\frac{(\lambda*\alpha*+1-\lambda)*\kappa*I_{sc}}{\alpha*I\alpha}\right)\right] \qquad (5)$$

#### 2.1.1 MPPT Control

To achieve steady-state operation the available dc-power PPV supplied by the solar arrays and the ac-power Pac fed into the grid must be balanced. The available dc-power depends on the environmental conditions and the array voltage. The inverter should always operate in the MPP to maximize the efficiency. To find the Maximum Power Point for all conditions a tracking method is used. Various MPPT techniques are described in [3].

MPPT techniques can be categorized into off-line and

on-line methods [4]. Off-line MPPT techniques require prior information about the PV array and measurements of either the solar irradiance, the short circuit current or the open circuit voltage of the particular PV array. An example of this is "fractional open-circuit voltage technique". The on-line MPPT methods include "hill climbing", "perturb and observe", "incremental conductance", and hybrid methods.

All the MPPT algorithms are designed to dynamically extract the maximum power from the PV panels. Usually, the condition $\partial p/\partial v=0$ is adopted to locate this operating point, since PV panels shows a unique global maximum power point. Generally, an MPPT algorithm varies the voltage Vdc according to the environmental conditions in order to keep the operating point of the PV panels close to MPP [5].

**2.2 Power Flow Model of PV System**

The model is obtained by taking into account the PV inverter output power limitations. Considering the ac side of the PV inverter, Fig. 2 represents the equivalent AC circuit. The inverter is represented as voltage and current source generator. $V_i^{\rho}$ is defined as the inverter three-phase ac output voltage and $V_g^{\rho}$ as the three-phase grid voltage. $I^{\rho}$ is the equivalent current injected to grid. $G^{\rho l}$ and $\beta^{\rho l}$ are the phase conductance and susceptance of the line connecting the grid and PV generator buses. Superscript $\rho$ and $l$ denotes the phases a, b, and c.

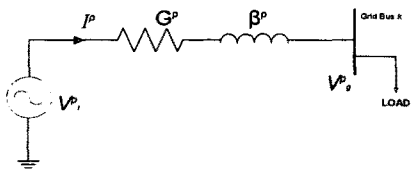


Fig. 2. AC side Equivalent Circuit

The expressions for the active and reactive power injected to the grid can be derived from the following complex power expressions:

$$S_{inj}^{\rho} = P_{inj}^{\rho} + \quad jQ_{inj}^{\rho} = V_g^{\rho *} \quad I_{inj}^{\rho} \tag{6}$$

After some arduous algebra, the equivalent active and reactive power expressions are deduced according to the following equations (7) where $\varphi$ is angle difference between phase voltages $V_i^{\rho}$ and $V_g^{\rho}$.

$$\begin{aligned} P_{inj}^{\rho} &= V_i^{\rho} V_g^{\rho} G^{\rho l} Cos\varphi - G^{\rho l} V_g^{\rho 2} + V_i^{\rho} V_g^{\rho} \beta^{\rho l} S\sin\varphi \\ Q_{inj}^{\rho} &= V_i^{\rho} V_g^{\rho} \beta^{\rho l} Cos\varphi - \beta^{\rho l} V_g^{\rho 2} - V_i^{\rho} V_g^{\rho} G^{\rho l} S\sin\varphi \end{aligned} \tag{7}$$

In power flow integration the PV system is modeled as controlled voltage and active power (P|V|) generator. For a lossless converter system, at steady state condition the active power PPV delivered by the PV arrays is equal to the active power output of the inverter. The apparent power capacity of the inverter $S_{i,\lim}^{\rho}$ is determined by multiplying the ac voltage output and ac current output of the inverter. The reactive power capacity of the inverter is limited by the $S_{i,\lim}^{\rho}$, therefore it is necessary to determine the maximum reactive power output of the inverter. The maximum reactive power limits can be calculated using the following relationship (8):

$$Q_{i,\lim}^{\rho} = \pm\sqrt{(S_i^{\rho})^2 - \quad (P_i^{\rho})^2} \tag{8}$$

Assuming the PV generator is connected in bus k, the total power demand for bus k is then calculated. The complex power model is defined as (9), where n is the total number of buses m connected to bus k.

$$S_k^{\rho} = V_k^{\rho *} \sum_{m=1}^{n} \sum_{l=a,b,c} Y_{km}^{\rho l} Y_{km}^{\rho l} V_m^{\rho} e^{j(\theta_m^l - \theta_k^{\rho})}$$

$$\begin{aligned} S_k^{\rho} = V_k^{\rho *} \sum_{m=1}^{n} \sum_{l=a,b,c} & (G_{km}^{\rho l} V_m^{\rho} Cos(\theta_m^l - \theta_k^{\rho}) + \beta_{km}^{\rho l} V_m^{\rho} Sin(\theta_m^l - \theta_k^{\rho})) \\ & + j(G_{mk}^{\rho l} V_m^{\rho} \sin(\theta_m^l - \theta_k^{\rho}) + \beta_{mk}^{\rho l} V_m^{\rho} Cos(\theta_m^l - \theta_k^{\rho})) \end{aligned} \tag{9}$$

Taking the imaginary part as the reactive power, $Q_k^{\rho}$ is calculated as (10):

$$Q_k^{\rho} = V_m^{\rho *} \sum_{m=1}^{n} \sum_{l=a,b,c} (G_{mk}^{\rho l} V_m^{\rho} \sin(\theta_m^l - \theta_k^{\rho}) + \beta_{mk}^{\rho l} V_m^{\rho} Cos(\theta_m^l - \theta_k^{\rho})) \tag{10}$$

Constraint:

$$Q_k^{\rho} \leq Q_{i,\lim}^{\rho}$$

The PV generator is then integrated with the power module in the standard manner a generator bus treated in the Newton-Raphson power flow method. When an iteration is completed a value for $Q_i^{\rho}$ is calculated and compared to $Q_{i,\lim}^{\rho}$. If the constraint is violated the P|V| generator is switch as PQ generator where the active and reactive power injected to the grid are then specified.

## 3. Simulation Results

A series of simulations were performed in different cases using the five-bus test network as shown in Fig. 3. The PV system is connected in bus 2 (P|V| bus), while the generator in bus 1 (slack bus) is a conventional type of generator.

Based on the five-bus system, tests under the following conditions have been carried out:

*Case 1:* The system is normal and the loads are balanced (base case).

*Case 2:* The System is normal while the loads are unbalanced.

*Case 3:* Load at bus 4 is doubled.

*Case 4:* As for case 3, but the line connecting bus 2 and 4 are trip off.

*Case 5:* Load at bus 5 is increased by 10% and the reactive power limit of PV generator was lowered to violate the constraints.

It can be observed from the results that the total power drawn by the two generators (1.7112 + j0.9082 pu) are enough for the total load demand (1.6 + j0.40 pu) of the system. From bus 1, (slack bus) large amount of reactive power was generated (0.9082 pu) and this amount is well excess by the total amount of reactive power drawn by the system loads (i.e. 0.4 pu). The PV generator in bus 2 draws the excess reactive power (0.6159 pu) Table 1.

When the load at bus 4 is doubled the generator 1 generates more active power to compensate the load increase while its reactive power generation was reduced, Table 2. In the first four cases imposed, results show (Table 1-4) that the voltage magnitudes in generator buses did not vary. In case 5, violation of the reactive power limit of the PV generator was done. The reactive power limit of the PV generator is slightly lowered, making the reactive power generation of the two generators lower than the total reactive power demand of the network load.

In order to compensate the total reactive power demand of the network load, the PV generator voltage is increased, Table 5.

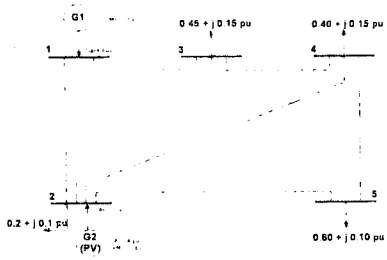


Fig. 3. Five-Bus Test Network

Table 1. Base Case Data

| Bus # | Phase | VM | VA | PGEN | QGEN |
|---|---|---|---|---|---|
| 1 | A | 1.06 | 0 | 1.3112 | 0.9082 |
| | B | 1.06 | 240 | 1.3112 | 0.9082 |
| | C | 1.06 | 120 | 1.3112 | 0.9082 |
| 2 | A | 1.00 | -2.0612 | 0.4 | -0.6159 |
| | B | 1.00 | 237.9388 | 0.4 | -0.6159 |
| | C | 1.00 | 117.9388 | 0.4 | -0.6159 |
| 3 | A | 0.9872 | -4.6367 | 0 | 0 |
| | B | 0.9872 | 235.3633 | 0 | 0 |
| | C | 0.9872 | 118.3633 | 0 | 0 |
| 4 | A | 0.9841 | -4.957 | 0 | 0 |
| | B | 0.9841 | 235.043 | 0 | 0 |
| | C | 0.9841 | 115.043 | 0 | 0 |
| 5 | A | 0.9717 | -5.7649 | 0 | 0 |
| | B | 0.9717 | 234.2351 | 0 | 0 |
| | C | 0.9717 | 114.2351 | 0 | 0 |

Table 2. *Case 2:* Unbalanced Load

| Bus # | Phase | VM | VA | PGEN | QGEN |
|---|---|---|---|---|---|
| 1 | A | 1.06 | 0 | 1.3245 | 0.9525 |
| | B | 1.06 | 240 | 1.2645 | 0.8978 |
| | C | 1.06 | 120 | 1.3805 | 0.8684 |
| 2 | A | 1.00 | -2.0245 | 0.4 | -0.6396 |
| | B | 1.00 | 238.1645 | 0.4 | -0.623 |
| | C | 1.00 | 117.5847 | 0.4 | -0.5626 |
| 3 | A | 0.982 | -4.6746 | 0 | 0 |
| | B | 0.9881 | 235.259 | 0 | 0 |
| | C | 0.9908 | 115.3763 | 0 | 0 |
| 4 | A | 0.9811 | -4.8404 | 0 | 0 |
| | B | 0.9831 | 234.9532 | 0 | 0 |
| | C | 0.9872 | 114.8792 | 0 | 0 |
| 5 | A | 0.9789 | -5.9574 | 0 | 0 |
| | B | 0.9755 | 235.2616 | 0 | 0 |
| | C | 0.9599 | 113.2259 | 0 | 0 |

Table 3. Load at bus 4 is doubled

| Bus # | Phase | VM | VA | PGEN | QGEN |
|---|---|---|---|---|---|
| 1 | A | 1.06 | 0 | 1.7428 | 0.8425 |
| | B | 1.06 | 240 | 1.7428 | 0.8425 |
| | C | 1.06 | 120 | 1.7428 | 0.8425 |
| 2 | A | 1.00 | -3.0911 | 0.4 | -0.4026 |
| | B | 1.00 | 236.9089 | 0.4 | -0.4026 |
| | C | 1.00 | 116.9089 | 0.4 | -0.4026 |
| 3 | A | 0.9758 | -6.5107 | 0 | 0 |
| | B | 0.9758 | 233.4893 | 0 | 0 |
| | C | 0.9758 | 113.4893 | 0 | 0 |
| 4 | A | 0.9701 | -7.2272 | 0 | 0 |
| | B | 0.9701 | 232.7728 | 0 | 0 |
| | C | 0.9701 | 112.7728 | 0 | 0 |
| 5 | A | 0.9666 | -7.2184 | 0 | 0 |
| | B | 0.9666 | 232.7816 | 0 | 0 |
| | C | 0.9666 | 112.7816 | 0 | 0 |

Table 4. *Case 4:* Line 2 to 4 is trip

| Bus # | Phase | VM | VA | PGEN | QGEN |
|---|---|---|---|---|---|
| 1 | A | 1.06 | 0 | 1.7633 | 0.9224 |
| | B | 1.06 | 240 | 1.7633 | 0.9224 |
| | C | 1.06 | 120 | 1.7633 | 0.9224 |
| 2 | A | 1.00 | -2.7342 | 0.4 | -0.378 |
| | B | 1.00 | 237.2658 | 0.4 | -0.378 |
| | C | 1.00 | 117.2658 | 0.4 | -0.378 |
| 3 | A | 0.9581 | -8.0489 | 0 | 0 |
| | B | 0.9581 | 231.9511 | 0 | 0 |
| | C | 0.9581 | 111.9511 | 0 | 0 |
| 4 | A | 0.9484 | -9.3139 | 0 | 0 |
| | B | 0.9484 | 230.6861 | 0 | 0 |
| | C | 0.9484 | 110.6861 | 0 | 0 |
| 5 | A | 0.9582 | -7.6724 | 0 | 0 |
| | B | 0.9582 | 232.3276 | 0 | 0 |
| | C | 0.9582 | 112.3276 | 0 | 0 |

Table 5. *Case 5:* Constraint Violated

| Bus # | Phase | VM | VA | PGEN | QGEN |
|---|---|---|---|---|---|
| 1 | A | 1.06 | 0 | 1.3627 | 0.2642 |
| | B | 1.06 | 240 | 1.3627 | 0.2642 |
| | C | 1.06 | 120 | 1.3627 | 0.2642 |
| 2 | A | 1.0304 | -2.7132 | 0.4 | (0.0001) |
| | B | 1.0304 | 237.2868 | 0.4 | (0.0001) |
| | C | 1.0304 | 117.2868 | 0.4 | (0.0001) |
| 3 | A | 1.103 | -5.0449 | 0 | 0 |
| | B | 1.103 | 234.951 | 0 | 0 |
| | C | 1.103 | 114.9551 | 0 | 0 |
| 4 | A | 1.0086 | -5.3974 | 0 | 0 |
| | B | 1.0086 | 234.6026 | 0 | 0 |
| | C | 1.0086 | 114.6026 | 0 | 0 |
| 5 | A | 0.9984 | -6.4537 | 0 | 0 |
| | B | 0.9984 | 233.5463 | 0 | 0 |
| | C | 0.9984 | 113.5463 | 0 | 0 |

## 4. Conclusions

Three phase power flow is commonly considered exclusively for the distribution systems, where single or double phase circuits may be present and loads may not always balanced between the three phases. In this paper the PV system was modeled in three-phase power flow by taking into consideration the PV inverter output power limitations. Different cases were carried out and results are presented.

## References


[1] E. I. rtiz-Revira and F. Peng, " A Novel Method to Estimate the Maximum Power for a Photovoltaic Inverter System" , *in Proc. 35th Annual IEEE Power Electronics Specialists Conference*,2004, pp. 2065-2069

[2] M. Djarallah and B. Azoui, "Grid Connected Interactive Photovoltaic Power Flow Analysis: A Technique for System Operation Comprehension and Sizing", in *Proc. 41st International Universities Power Engineering Conference*, 2006, pp. 69-73

[3] T. Esram and P. Chapman, "Comparison of Photovoltaic Array Maximum Power Point Tracking Techniques", *IEEE Transactions on Energy Conversion*, 2007, pp. 439-449

[4] C. W. Tan, T. C. Green and C. A. Hernandez-Aramburo, "An Improved Maximum Power Point Tracking Algorithm with Current-Mode Control for Photovoltaic Applications", *in Proc. International Conference on Power Electronic and Drives Systems*, 2005, pp. 489-494

[5] G. Grandi, C. Rossi and D. Casadei, "A MPPT Algorithm for Single-Phase Single-Stage Photovoltaic Converters", *IFAC 2005*

[6] B. Bekker and H. J. Beukes, "Finding an Optimal PV Panel Maximum Power Point Tracking Method", in *Proc. 7th AFRICON Conference in Africa*, 2004, pp. 1125-1130

[7] E. Acha, C. R. Fuerte-Esquivel, H. Ambriz-Perez and C. Angeles-Camacho, "FACTS Modelling and Simulation in Power Networks"